PHYSICAL REVIEW D **89,** 053012 (2014)

Anomalous Higgs-boson coupling effects in HW^+W^- production at the LHC

Emidio Gabrielli,[1,2,*] Matti Heikinheimo,[1] Luca Marzola,[3] Barbara Mele,[4] Christian Spethmann,[1] and Hardi Veermäe[1,3]

[1]*National Institute of Chemical Physics and Biophysics, Rävala 10, 10143 Tallinn, Estonia*

[2]*INFN, Sezione di Trieste, Via Valerio 2, 34127 Trieste, Italy*

[3]*Laboratory of Theoretical Physics, Institute of Physics, University of Tartu, Tähe 4, 51010 Tartu, Estonia*

[4]*INFN, Sezione di Roma, Piazzale Aldo Moro 2, 00185 Roma, Italy*

(Received 26 December 2013; published 25 March 2014)

We study the LHC associated production of a Higgs boson and a W^+W^- vector-boson pair at 14 TeV, in the standard model and beyond. We consider different signatures corresponding to the cleanest H and W decay channels and discuss the potential of the high-luminosity phase of the LHC. In particular, we investigate the sensitivity of the HW^+W^- production to possible anomalous Higgs couplings to vector bosons and fermions. Since the b-quark initiated partonic channel contributes significantly to this process, we find a moderate sensitivity to both the size and sign of an anomalous top-quark Yukawa coupling, because perturbative unitarity in the standard model implies a destructive interference in the $b\bar{b}$ subprocess. We show that a combination of various signatures can reach ∼9 standard-deviation sensitivity in the presently allowed negative region of the top-Higgs coupling, if not previously excluded.

DOI: 10.1103/PhysRevD.89.053012 PACS numbers: 14.80.Bn, 12.60.Fr, 12.60.-i, 14.65.Ha

I. INTRODUCTION

Since the Higgs boson discovery [1,2] in 2012, the major experimental task at the LHC is to test the detailed standard model (SM) predictions for the new-particle properties and couplings to known particles. Possible nonstandard Higgs couplings to both known and speculated particles are to be taken into account in Higgs studies. In order to characterize the Higgs boson in the most accurate way, one should then scrutinize not only the main Higgs production channels but also the rarest processes that can be sensitive to anomalous and/or new kinds of interactions. Here, we consider the associated production of a Higgs boson and a vector boson pair in the channel[1]

$$pp \to HW^+W^-. \tag{1}$$

The cross section for the process in Eq. (1) is of third order in the electroweak coupling, just like the dominant Higgs boson production in WW fusion. On the other hand, the phase-space factor for the production of three massive objects depletes the total production rate at 14 TeV down to about 8 fb [at leading order (LO)] [4,5], compared with the WW/ZZ-fusion cross section of about 4 pb. Next-to-leading order (NLO) QCD corrections enhance the HW^+W^- rates by about 50% [6]. Similar considerations hold for the cross sections corresponding to the HWZ and HZZ final states, which are further depleted by SU(2) invariance down to about 4 and 2 fb at LO, respectively. The study of such relatively small cross-section processes then requires the large integrated luminosities expected in the high-luminosity phase of the LHC (HL-LHC), where one expects to collect about 3000 fb^{-1} of data per experiment.

It is well known that, in presence of anomalous Higgs couplings to vector bosons $V = W$, Z and/or fermions f, there are processes which violate perturbative unitarity at high energies. In particular, any measured deviation from the SM VVH and $f\bar{f}H$ couplings results in new phenomena, since further unknown degrees of freedom are necessarily required in order to recover unitarity in $V_LV_L \to V_LV_L$ [7] and $V_LV_L \to f\bar{f}$ scatterings [8].

Presently, ATLAS [9,10] and CMS [11] data show a sign ambiguity in the Higgs couplings to fermions. The two-dimensional fits of $C_V = g_{VVH}/g^{\rm SM}_{VVH}$ and $C_f = g_{ffH}/g^{\rm SM}_{ffH}$ (where g_{HVV} and g_{ffH} parametrize the Higgs couplings to gauge bosons and fermions, respectively) are both compatible within 2σ with a SM coupling setup $C_V = C_f = 1$. On the other hand, a non-SM fit with $C_V \simeq -C_f \simeq 1$ is not yet excluded [10]. The relative sign between the VVH and $f\bar{f}H$ couplings is predicted by the SM (being related to the SM Higgs mechanism for the fermion mass generation), and a flipped sign would spoil the unitarity and renormalizability of the theory. Nevertheless, there are theoretical frameworks that predict such a possibility [12,13].

A possible strategy to resolve the above sign degeneracy in the LHC data is to look at processes where two contributions to the scattering amplitude, depending separately on the VVH and $f\bar{f}H$ couplings, interfere. An example is given by the Higgs production in association with a single top in $pp \to tqH$, whose total cross section gets largely enhanced by flipping the top Yukawa coupling

[*] On leave from Department of Physics, University of Trieste, Strada Costiera 11, I-34151 Trieste, Italy.

[1] The Higgs boson production in association with a pair of electroweak gauge bosons $(WW, ZZ, Z\gamma)$ in e^+e^- collisions has been considered in the SM framework in [3].

 © 2014 American Physical Society

sign in such interference contributions [14–16]. This gives the process a considerable potential for constraining the negative $C_f \simeq -C_V$ coupling region [17,18]. Indeed, even the present $7+8$ TeV LHC data set could be sufficient to exclude the wrong-sign Yukawa solution in $pp \to tqH$ [19]. The large enhancement (by about a factor of 13 at the LHC energies) resulting from the flipped Yukawa sign in the $pp \to tqH$ cross section points to unitarity breaking at large energies [18]. Nevertheless, this cross section can be reliably computed at the LHC even in the anomalous coupling region, since perturbative unitarity breaks at energies of the $bW \to tH$ subprocess above 10 TeV [18].

The larger data sample on Higgs-boson production, expected at the LHC in forthcoming years, will have an enormous potential to check whether the actual couplings of the newly observed particle indeed approach the corresponding SM Higgs interactions, or show some deviation from them [20,21].

In the present analysis, we aim also to analyze what the study of $pp \to HW^+W^-$ can add to the potential of other Higgs production processes characterized by higher cross section. This is motivated by the fact that in $pp \to HW^+W^-$, the partonic contribution arising from the b-quark scattering $b\bar{b} \to HW^+W^-$ (Fig. 1) provides another example of process sensitive to the top Yukawa sign (and magnitude) through the interference between diagrams where the Higgs boson is radiated by a W/Z boson and those ones where it is emitted by an internal top-quark line. Even in this case, anomalous Higgs couplings will induce perturbative unitarity violations. Nevertheless, the possible impact of such violations on the total cross section will be diluted by the dominant light-quark scattering contribution to the $pp \to HW^+W^-$ cross section, which is mostly insensitive to the Higgs Yukawa couplings. In the following, we will discuss the $pp \to HW^+W^-$ rate

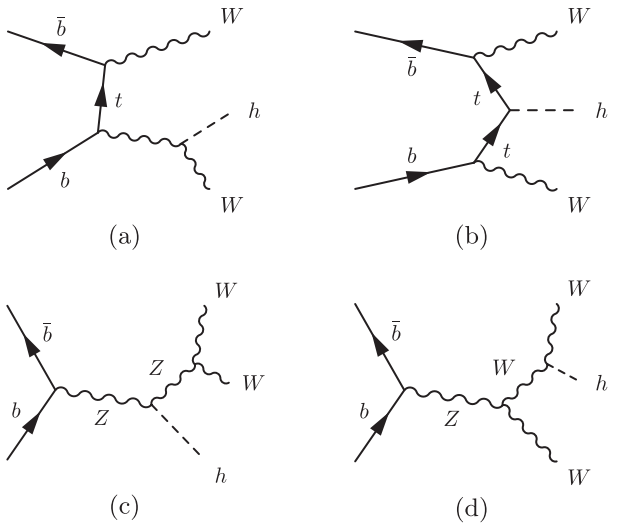

FIG. 1. Classes of Feynman diagrams (a), (b), (c), and (d) for the partonic $b\bar{b} \to HW^+W^-$ process.

sensitivity to both Higgs Yukawa and gauge couplings, and analyze the corresponding unitarity bounds in the presence of anomalous couplings.

The paper is organized as follows. In Sec. II, within the SM framework, we evaluate the $pp \to HW^+W^-$ total cross section for different c.m energies, and compare it to the cross sections for other multiboson final states. In Sec. III, we discuss signal versus background expectations at the HL-LHC, for the most robust HW^+W^- signatures (i.e., multileptons final states, and diphoton resonances). Then, in Sec. IV, we discuss the sensitivity of the HW^+W^- production to anomalous Higgs couplings to fermions and vector bosons. In Sec. V, we sum up and give our conclusions.

II. TRIBOSON CROSS SECTIONS

In order to provide a context for our study, we start by giving an overview of the triboson electroweak final states that involve at least one Higgs boson for the LHC energies and beyond. In particular, we compare the $pp \to HW^+W^-$ cross section to the ones for other triboson final states, including either one or two Higgs bosons, at different collision c.m. energies that could be of interest at future pp colliders [22]. The HH production cross sections are also presented here for comparative purposes. We postpone to the next section a detailed study of the cleanest HW^+W^- production signatures versus the most relevant backgrounds, and a discussion of the potential of the HL-LHC to observe the HW^+W^- process with an integrated luminosity of 3000 fb^{-1}.

In Table I we present the total cross sections for HW^+W^-, HWZ, HZZ, HHW, HHZ, and HH production in proton-proton collisions for the LHC design energy of 14 TeV, and at possible future hadron colliders. From now on, we will assume $m_H = 125$ GeV.

The LO cross sections in Table I have been computed with MadGraph5 [23], by using the CTEQ6L1 parton distribution functions (PDF's) [24]. The HHW and HHZ cross sections have been calculated by retaining only the tree-level contribution of vector boson fusion (VBF) from quarks initiated processes, and by neglecting the next-to-leading contribution arising from W/Z radiation by a HH pair produced via gluon-gluon fusion. The dependence on

TABLE I. LO electroweak triboson cross sections (including either one or two Higgs bosons in the final state), in pp collisions (in fb) for $m_H = 125$ GeV, at different c.m. energies, and, for comparison, the NLO cross section for $gg \to HH$.

	14 TeV	33 TeV	40 TeV	60 TeV	80 TeV	100 TeV
HW^+W^-	8.4	29	38	65	94	124
HWZ	3.8	14	18	31	44	58
HZZ	2.1	7.4	9.6	16	24	31
HHW	0.43	1.6	2.1	3.6	5.2	7.0
HHZ	0.27	1.0	1.3	2.2	3.3	4.4
HH	33.8	207	298	609	980	1420

the renormalization and factorization scales has been tested by varying the scale from a central value $\mu_0 = 265$ GeV $\approx 2M_W + M_H$ to $2\mu_0$ and $\mu_0/2$. The corresponding scale uncertainty has been found in the range 1%–2%. For comparison, we also include in Table I the NLO gluon fusion cross section for HH production [22].

The HW^+W^- production (from now on labeled just as HWW) turns out to have the largest cross section among all triboson channels involving Higgs bosons in the final state. Its production rate is almost a factor of 4, or 11, smaller than the double Higgs production at 14, or 100 TeV, respectively. Notice that the HH cross section increases with energy faster than all triboson cross sections, as the latter acquire almost a common rescaling factor while growing with energy. This behavior reflects the different evolution in energy of the gluon PDF (that mainly influences the HH production) versus the quark PDFs, which give the dominant contribution to the triboson cross sections.

III. HWW SIGNALS AND BACKGROUNDS

In this section, we detail our analysis of signatures and corresponding backgrounds for the cleanest HWW decay channels. Note that the present study partially overlaps with the analysis of the $HH \to HWW^*$ final state mediated by two Higgs-boson production [25], which has a slightly larger cross section ($\sigma_{HH} \times 2BR(H \to WW^*) \sim 16$ fb at 14 TeV), but differs in the presence of one "less characterizing" off-shell W in the final state.

Table II shows a list of the most relevant final states arising from the HWW system decays, as well as the corresponding event numbers at 14 TeV for 3000 fb^{-1} (before applying any kinematical cut). One can see how multilepton and two-photon final states (that are the most robust against background) are in general characterized by lower rates.

In the following, both signal and background event numbers have been worked out by using MadGraph 5 [23], interfaced with Pythia 6.4 [26] for decays with large particle multiplicities. All event samples have been analyzed at parton level. The following set of basic kinematical cuts has been universally applied in this paper:

(i) for final state leptons (e, μ) and photons, we require a pseudo-rapidity cut $|\eta| < 2.5$, and a transverse momentum cut $p_T > 10$ GeV;

(ii) for final state quark and gluon jets, we impose $|\eta| < 2.5$ and $p_T > 20$ GeV. We disregard forward jets with $|\eta| > 2.5$ to ensure that b jets can be more reliably identified, b-tagging algorithms being more efficient in the central part of the detector. We assumed a b-jet detection efficiency of 70%;

(iii) for each pair of visible objects (i, j), we require an isolation cut $\Delta R_{ij} > 0.4$, where $\Delta R_{ij} = \sqrt{\eta_{ij}^2 + \phi_{ij}^2}$, and $\eta_{ij}(\phi_{ij})$ is their rapidity (azimuthal) separation.

In order to investigate hadronic tau decays, we have modified the Tauola code in MadGraph to assign a unique particle identifier to the hadronic tau decay products, $\tau_{\rm had}$. We then applied to $\tau_{\rm had}$ the same set of cuts as adopted for quark and gluon jets.

In our analysis, we do not include decay channels into N jets plus two opposite-sign leptons, or one single lepton, or no leptons, which are dominated by QCD backgrounds such as top-pair production. This excludes the highest-rate (but challenging) channels with Higgs into $b\bar{b}$.[2] We also disregard

TABLE II. List of most relevant final states arising from the HWW system decays, and the corresponding event numbers at 14 TeV for 3000 fb^{-1}, before applying any kinematical cut. Here ab stands for the unity of attobarn.

$H \to$	Final state	BR	ev/3 ab^{-1}	Signature
$b\bar{b}$		61%	16800	
	$b\bar{b}\ \ell\nu\ \ell\nu$	2.9%	815	$2b\ 2\ell\ \not{E}_T$
	$b\bar{b}\ \ell\nu\ jj$	18%	4960	$2b\ 2j\ \ell\ \not{E}_T$
	$b\bar{b}\ jj\ jj$	27%	7560	$2b\ 4j$
WW^*		20%	5580	
	$\ell\nu\ \ell\nu\ \ell\nu\ \ell\nu$	0.047%	13	$4\ell\ \not{E}_T$
	$\ell\nu\ \ell\nu\ \ell\nu\ jj$	0.58%	159	$2j\ 3\ell\ \not{E}_T$
	$\ell\nu\ \ell\nu\ jj\ jj$	2.6%	727	$4j\ 2\ell\ \not{E}_T$
	$\ell\nu\ jj\ jj\ jj$	5.3%	1480	$6j\ \ell\ \not{E}_T$
	$jj\ jj\ jj\ jj$	4.1%	1120	$8j$
$\tau^+\tau^-$		6.2%	1710	
	$\ell\nu\bar{\nu}\ \ell\nu\bar{\nu}\ \ell\nu\ \ell\nu$	0.033%	9	$4\ell\ \not{E}_T$
	$\ell\nu\bar{\nu}\ \ell\nu\bar{\nu}\ \ell\nu\ jj$	0.20%	55	$2j\ 3\ell\ \not{E}_T$
	$\ell\nu\bar{\nu}\ \ell\nu\bar{\nu}\ jj\ jj$	0.30%	84	$4j\ 2\ell\ \not{E}_T$
	$\ell\nu\bar{\nu}\ \tau_{\rm had}\ \ell\nu\ \ell\nu$	0.13%	37	$\tau_{\rm had}\ 3\ell\ \not{E}_T$
	$\ell\nu\bar{\nu}\ \tau_{\rm had}\ \ell\nu\ jj$	0.81%	223	$2j\ \tau_{\rm had}\ 2\ell\ \not{E}_T$
	$\ell\nu\bar{\nu}\ \tau_{\rm had}\ jj\ jj$	1.2%	340	$4j\ \tau_{\rm had}\ \ell\ \not{E}_T$
	$\tau_{\rm had}\ \tau_{\rm had}\ \ell\nu\ \ell\nu$	0.13%	37	$2\tau_{\rm had}\ 2\ell\ \not{E}_T$
	$\tau_{\rm had}\ \tau_{\rm had}\ \ell\nu\ jj$	0.82%	226	$2\tau_{\rm had}\ 2j\ \ell\ \not{E}_T$
	$\tau_{\rm had}\ \tau_{\rm had}\ jj\ jj$	1.2%	345	$2\tau_{\rm had}\ 4j$
ZZ^*		2.5%	690	
	$\ell\ell\ \ell\ell\ \ell\nu\ \ell\nu$	0.001%	0	$6\ell\ \not{E}_T$
	$\ell\ell\ \ell\ell\ \ell\nu\ jj$	0.003%	1	$2j\ 5\ell\ \not{E}_T$
	$\ell\ell\ \ell\ell\ jj\ jj$	0.005%	1	$4j\ 4\ell$
	$\ell\ell\ jj\ \ell\nu\ \ell\nu$	0.006%	2	$2j\ 4\ell\ \not{E}_T$
	$\ell\ell\ jj\ \ell\nu\ jj$	0.017%	5	$4j\ 3\ell\ \not{E}_T$
	$\ell\ell\ jj\ jj\ jj$	0.053%	15	$6j\ 2\ell$
	$jj\ jj\ \ell\nu\ \ell\nu$	0.059%	16	$4j\ 2\ell\ \not{E}_T$
	$jj\ jj\ \ell\nu\ jj$	0.36%	100	$6j\ \ell\ \not{E}_T$
	$jj\ jj\ jj\ jj$	0.55%	152	$8j$
$\gamma\gamma$		0.22%	61	
	$\gamma\gamma\ \ell\nu\ \ell\nu$	0.011%	3	$2\gamma\ 2\ell\ \not{E}_T$
	$\gamma\gamma\ \ell\nu\ jj$	0.065%	18	$2\gamma\ 2j\ \ell\ \not{E}_T$
	$\gamma\gamma\ jj\ jj$	0.099%	27	$2\gamma\ 4j$

[2]The $WWb\bar{b}$ channel has been proposed as a signal channel for HH production [25]. In this case the presence of two on-shell Higgs bosons (implying at least one very off-shell W) provides additional kinematic constraints to reject the top background.

the Higgs decay into ZZ^* that generates too few events into the most-robust semileptonic/all-leptonic final states.

A. Four lepton final states

HWW final states can go to four charged leptons either via $H \to WW^* \to \ell\nu\ell\nu$, or via $H \to \tau^+\tau^- \to \ell\nu\nu\ell\nu\nu$, with the accompanying on-shell W pair also decaying leptonically, $WW \to \ell\nu\ell\nu$. In either cases, there is significant missing energy due to either four or six neutrinos. The main irreducible backgrounds for these channels are

(i) EW continuum production of four W's, all decaying leptonically
(ii) WWZ with Z decaying into either ee, $\mu\mu$, or two leptonically decaying τ's. The former channel has higher rates, but can be tamed by cutting away the Z mass region from the lepton pair invariant mass distribution (indeed we do not include any background presenting a $Z \to ee, \mu\mu$ resonance throughout the present analysis). The leptonic Z decay via $\tau^+\tau^-$ (that we include) has lower rates, but is less characterized, and in general more overlapped with the Higgs signal into leptons
(iii) ZZ pairs with the Z's decaying into e, μ leptons or leptonically decaying taus; again the decays $Z \to \ell^+\ell^-$ can be cut away by reconstructing the Z resonance
(iv) ZH with Z decaying into e, μ leptons or leptonically decaying taus, and H decaying to leptons through WW^* or taus pairs
(v) HH with both H's going into WW^*, followed by leptonic decays of the W bosons.

The corresponding signal and background rates are shown in Table III. We find that the most dangerous irreducible background, after our basic kinematic cuts, comes from ZZ production, with both Z's decaying into τ's. In order to reduce this background, we cut on the scalar sum of the missing energy and the transverse momentum of the four leptons, $\sum_i p_T^{\ell_i} + \not{E}_T$. Indeed, leptons from the indirect decays via $\tau \to \ell\nu\nu$ are typically produced with lower transverse energy. The total missing energy in the event is also lower for indirect decays, since the eight neutrinos in each event are on average emitted in random directions on the transverse plane, and their momenta partially cancel each other out. We find that, by applying a lower cut of 200 GeV on $\sum_i p_T^{\ell_i} + \not{E}_T$, the ZZ background can be reduced by about a factor of 10, while the signal falls only by 25%.

After all the cuts described above, the signal to background ratio is close to 0.32, and the corresponding significance ($S/\sqrt{S+B}$ in unity of standard deviation σ_S) of the four-lepton channel for a data set of 3000 fb^{-1} is about $1.3\sigma_S$.

TABLE III. Signal and background cut flow for $4\ell + \not{E}_T$ final states. All cross sections are in ab. In the third column, $\sum p_T + \not{E}_T$ labels the cut on the scalar sum of missing energy and four-lepton transverse momenta, $\sum_i p_T^{\ell_i} + \not{E}_T > 200$ GeV.

	Basic cuts	$\sum p_T + \not{E}_T$
HWW signal:		
via $H \to WW^*$	2.1	1.6
via $H \to \tau\tau$	1.0	0.8
$ZZ \to 4\tau \to 4\ell + \nu's$	17.9	1.7
WWZ	3.3	2.5
$4W$	0.7	0.7
ZH, $H \to WW^*$	0.7	0.2
ZH, $H \to \tau\tau$	1.6	0.4
$HH \to WW^*WW^*$	3.1	2.1
Total signal	3.1	2.4
Total background	27.3	7.6

B. Hadronic $W + 3$ leptons

We will now investigate the channel with one hadronic W decay ($W_{\rm had}$) plus three charged leptons in the final state. As in the previous channel, this signature can arise from the HWW state in connection to two different Higgs decays. For the Higgs decaying into WW^*, compared to the four-lepton final state, the rate is enhanced by the following two effects:

(i) the W branching ratio (BR) into hadrons is more than a factor of 3 larger than the one into $e\nu + \mu\nu$;
(ii) any of the three on-shell W's can decay hadronically, giving a further factor of 3 from combinatorial enhancement.

On the other hand, when the signature arises from $H \to \tau\tau \to$ leptons, the W BR is again increased by a factor of 3, while the combinatorial factor is only 2. Altogether, after applying kinematical cuts, about 80% of the signal events originates from the $H \to WW^*$ decay mode (cf., Table IV).

TABLE IV. Signal and background cut flow in the $3\ell + W_{\rm had}$ final states. All cross sections are in ab. The cut labeled $m(W)$ requires the invariant mass of the two jets to satisfy $75.4 < m^{jj} < 85.4$ GeV.

	Basic cuts	$m(W)$
HWW signal:		
via $H \to WW^*$	22.3	18.8
via $H \to \tau\tau$	4.3	4.3
WWZ	17.7	17.7
$4W$	7.0	7.0
$jjWWW$	740	29.4
$jjWZ$	1540	49.9
$jjWH$, $H \to WW^*$	169	9.7
$jjWH$, $H \to \tau\tau$	82.2	4.4
$t\bar{t}W$	825	34.9
$t\bar{t}Z$	11.7	0.5
$HH \to WW^*WW^*$	10.3	5.4
Total signal	26.6	23.1
Total background	3400	159

We will now discuss the (mostly irreducible) backgrounds that can lead to the $W_{\rm had} + 3\ell + \not{E}_T$ final state, in order of relevance:

(i) 2 jets + WZ, where the Z decays via τ's to leptons. The total rate for this background after basic kinematic cuts is larger than 1 pb. On the other hand, by requiring the jet pair to reconstruct the W mass, it falls down by a factor 20;

(ii) $t\bar{t}W$ production, where the two b jets from top decays are mistagged as light jets and reconstruct the W mass. By demanding the jets to reconstruct the W mass within 5 GeV, the $t\bar{t}W$ background has been reduced by a factor ∼24 (cf., Table IV). Similarly, the $t\bar{t}Z$ production, for $Z \to \ell\ell$, can contribute to the background whenever one of the charged leptons from the Z decay falls outside the experimental acceptance (this actually occurs in about $1/6$ of the events);

(iii) further QCD backgrounds originate from $jjWWW$ and $jjWH$, but can similarly be reduced by requiring the jet-pair invariant mass to reconstruct M_W;

(iv) purely electroweak backgrounds, which mainly originate from $4W$ and WWZ production. For WWZ, we assume that the Z decays via τ's to leptons;

(v) $HH \to WW^*WW^*$ production. Note that HH is more affected by previous cuts, since two out of four W's are off-shell, and, for W hadronic decays, do not reconstruct M_W, while, for W leptonic decays, give reduced transverse momenta.

Then, in general, in addition to our basic kinematic cuts, we demand the two jets to reconstruct M_W within a mass window of ±5 GeV. The effect of the above cuts on signal and background is shown in Table IV. With 3000 fb^{-1}, we expect 69 signal and 477 background events. The S/B ratio is 0.145 and the corresponding significance is $3.0\sigma_S$.

C. Higgs decay into diphotons

We now examine the final states where the Higgs decays to two photons. The resonant $\gamma\gamma + WW$ signal is very clear, and the backgrounds are in general small, but the signal is penalized by the small Higgs BR to photons. The cleanest signature to look for would obviously be the full leptonic WW final state, but the corresponding rate is highly suppressed, giving a total of about three events with 3000 fb^{-1} (cf., Table II). Thus we concentrate on the larger-rate semileptonic WW channel, resulting in the final state $jj\ell\nu\gamma\gamma$. The main irreducible backgrounds are

(i) $jjW\gamma\gamma$, with the W decaying into leptons, where the jets reconstruct the W mass, and the photons reconstruct the Higgs mass;

(ii) $jjWH$, that is WH associated production with two extra jets faking a hadronic W decay;

(iii) $WW\gamma\gamma$, with one W decaying leptonically, and the other one hadronically, and two radiated photons that reconstruct the Higgs system;

TABLE V. The cut-flow for the 2 jets + $1\ell + 2\gamma$ final states. All cross sections are in ab. The labels are defined as follows: $m(H)$ stands for a cut on the $\gamma\gamma$ invariant mass, 123 GeV < $m^{\gamma\gamma}$ < 127 GeV, Σp_T^{γ} is a cut on the scalar sum of the photon transverse momenta, $p_T^{\gamma_1} + p_T^{\gamma_2} > 100$ GeV, $m(W)$ is a cut on the jet-pair invariant mass, 75.4 GeV < m^{jj} < 85.4 GeV, and Σp_T^{j} is a cut on the scalar sum of the jet transverse momenta, $p_T^{j_1} + p_T^{j_2} > 70$ GeV.

	Basic cuts	$m(H)$	Σp_T^{γ}	$m(W)$	Σp_T^{j}
HWW signal	2.5	2.5	2.3	2.0	1.95
$jjW\gamma\gamma$	18400	144	105	4.3	4.1
$jjWH$	61	61	55	3.1	2.5
$WW\gamma\gamma$	264	2.4	1.7	1.5	1.4
HH	2.0	2.0	1.8	1.22	1.18
Total signal	2.5	2.5	2.3	2.0	1.95
Total background	18700	209	164	10.1	9.2

(iv) HH, with one of the Higgs bosons decaying into two photons and the other one into a semileptonic W pair. One of the W's from the Higgs decay being off-shell, this background will be reduced by a proper cut around M_W on the hadronic W^*.

The two-jet and two-photon invariant masses are then required to be within the ranges $M_W \pm 5$ GeV, and $m_H \pm 2$ GeV, respectively. The main backgrounds contain radiated jets faking the W, and/or radiated photons faking the Higgs. The p_T spectrum of the radiated objects is softer than the corresponding spectrum for the decay products of a real W and Higgs, so we require additional cuts on the scalar p_T sum of the two jets and the two photons, respectively, as $p_T^{j_1} + p_T^{j_2} > 70$ GeV and $p_T^{\gamma_1} + p_T^{\gamma_2} > 100$ GeV. The effect of the above cuts on signal and background is shown in Table V. As a results, one gets a $jj\ell\nu\gamma\gamma$ signal to background ratio of about $2/9$, and a significance $\simeq 1.0\sigma_S$ for a dataset of 3000 fb^{-1}.

D. Same sign leptons from $H \to \tau\tau$

We now discuss the $\ell\nu jj\tau\tau$ final state, arising from semileptonic WW decays, and Higgs decaying to τ pairs. We consider the case where one of the taus decays leptonically, and the other hadronically, and demand two same-sign leptons (one from a W and one from a τ). The signature is therefore two jets, two same-sign leptons, and one hadronic tau ($\tau_{\rm had}$). We select the latter channel since same-sign lepton events are very much suppressed in the SM, so that even a small number of signal events could lead to an observation.

The main irreducible backgrounds for this signature are

(i) WWZ, with $Z \to \tau\tau$. Because of the missing energy from neutrinos in tau decays, the mass of the particle decaying to taus can not be reconstructed accurately, and the Z and Higgs signals will be in general quite overlapped;

(ii) $jjWH$, i.e., WH associated production with two extra jets, and $H \to \tau\tau$;

TABLE VI. The cut-flow for the 2 jets $+ \ell^{\pm}\ell^{\pm} + \tau_{\rm had}$ final states. All cross sections are in ab. The label $m(W)$ stands for a cut on the jet-pair invariant mass, 75.4 GeV $< m^{jj} <$ 85.4 GeV.

	Basic cuts	$m(W)$
HWW signal	5.6	5.6
WWZ	27.6	27.6
$jjWH$	106	7.7
$jjWZ$	2820	129
Total signal	5.6	5.6
Total background	2950	164

(iii) $jjWZ$, with $Z \to \tau\tau$. This is the main background for this channel because of the large production cross section. Again, the Z and Higgs decay products via taus will be in general quite overlapped.

In addition to our basic kinematic cuts, we again demand the two-jet mass to be within the range $M_W \pm 5$ GeV, and assume 100% efficiency for hadronic tau identification. The effect of kinematical cuts on the signal and background is shown in Table VI. After all cuts, the same-sign lepton signal to background ratio for $\ell\nu jj\tau\tau$ is about 0.034, and the significance for a data set of 3000 fb^{-1} is $0.74\sigma_S$.

E. Same sign leptons from $H \to W^+W^-$

The same sign dilepton signal can also arise from $W^+W^-H \to W^+W^-W^+W^-$, where the positively charged W's decay to leptons and the negatively charged W's into hadrons or vice versa. In this case the final state consists of two hadronic W systems, two same sign leptons, and missing energy. The most relevant backgrounds are

(i) $4jW^{\pm}W^{\pm}$, where the W's decay into leptons, and the four jets fake the two hadronic W's. Because of the valence-quark charge distribution, the cross section of the positively charged W pair production is about three times as large as the negative pair one.

(ii) $jjW^{\pm}W^{\pm}W^{\mp}$, where the same sign W's decay into leptons, and the opposite sign W decays into hadrons, and the two jets reconstruct the remaining hadronic W.

(iii) $t\bar{t}W^{\pm} \to b\bar{b}W^+W^-W^{\pm}$, where the same sign W's decay into leptons and the opposite sign W decays into hadrons, and the two b jets fake the hadronic W.

(iv) $tW^+W^-j \to W^+bW^+W^-j$, or the charge conjugate process, where the same sign W's decay into leptons and the opposite sign W into hadrons, and the b jet plus the light jet fake the hadronic W.

(v) $W^+W^+W^-W^-$, that is electroweak production of four W bosons, with hadronic (leptonic) decays of the positively (negatively) charged W's, or vice versa.

To extract the signal from the background we require the four jets in the final state to combine into two pairs with invariant mass within ± 5 GeV around M_W. To reduce the background from the $t\bar{t}W$ production, events with b-tagged jets are vetoed, (assuming a 70% tagging efficiency).

TABLE VII. The cut-flow for four jets $+ \ell^-\ell^-$ final state. All cross sections are in ab. The label $m(W)$ stands for the cut on the invariant mass of the two jet pairs, 75.4 GeV $< m^{jj} <$ 85.4 GeV. The event passes the $m(W)$ cut for any possible combination of the two pair systems built from the four jets, where both pairs pass the cut.

	Basic cuts	$m(W)$
HWW signal	4.3	2.7
$4jWW$	828	2.5
$2jWWW$	406	18.2
$t\bar{t}W$	138	7.7
$tWWj$	112	2.5
$WWWW$	0.3	0.3
Total signal	4.3	2.7
Total background	1480	31.2

TABLE VIII. Same as in Table VII for four jets $+ \ell^+\ell^+$ final states.

	Basic cuts	$m(W)$
HWW signal	4.3	2.7
$4jWW$	2830	14.2
$2jWWW$	679	30.2
$t\bar{t}W$	262	12.9
$tWWj$	249	6.2
$WWWW$	0.3	0.3
Total signal	4.3	2.7
Total background	4020	63.8

The resulting signal and background rates are shown in Table VII for negatively charged leptons and in Table VIII for positively charged leptons. Because of the valence-quark charge distribution, the background cross sections are generally smaller for the negatively charged lepton pair, and hence this channel is more significant. After cuts, the signal to background ratio is 0.087 (0.042) for negative (positive) sign leptons, and the combined significance for 3000 fb^{-1} is 0.98σ.

F. Further relevant backgrounds

The associated production of a Higgs boson and a $t\bar{t}$ pair gives a common background for all final states investigated above, since the final state $Ht\bar{t} \to HWWb\bar{b}$ can mimic the signal HWW whenever the final b jets are not reconstructed.

The LO cross section for the process $pp \to Ht\bar{t} \to HWWb\bar{b}$ is about 360 fb at $\sqrt{S} = 14$ TeV. If we require, in a parton-level simulation, that the b jets have transverse momentum $p_T > 20$ GeV and pseudorapidity $|\eta| < 4.5$ to be reconstructed at least as further light jets, then both b jets will be reconstructed in 91.9% of the events, and at least one b jet will be reconstructed in 99.75% of the events. Thus the $Ht\bar{t}$ background can be effectively suppressed down to 0.25% of the original cross section by a veto on any additional jets with $p_T > 20$ GeV and $|\eta| < 4.5$. Then,

TABLE IX. Signal versus background rates (in ab) after all dedicated cuts for different final states, and the corresponding significance in unity of σ_S ($S/\sqrt{S+B}$) for 3000 fb^{-1}. The total significance of $3.6\sigma_S$ is the sum in quadrature of all individual significances.

Final state	Signal	Background	$S/\sqrt{S+B}$
$4\ell + \not{E}_T$	2.4	7.6	1.3
$3\ell + 2j$	23.1	159	3.0
$1\ell + 2j + 2\gamma$	1.95	9.2	1.0
$\ell^\pm\ell^\pm + 2j + \tau_{\rm had}$	5.6	164	0.74
$\ell^-\ell^- + 4j$	2.7	31.2	0.80
$\ell^+\ell^+ + 4j$	2.7	63.8	0.57
Total			3.6

the latter acceptance cuts reduce the cross section of the $t\bar{t}H$ background to about 0.9 fb, before applying the relevant BR's for the Higgs and W bosons for each final state. On the other hand, the inclusion of extra QCD radiation and shower effects will in general impact the present conclusion.

A further potentially dangerous background for the $W_{\rm had} + 3\ell$ signal is the $t\bar{t}j \to 2\ell 2\nu b\bar{b}j$ production, where a b jet is mistagged as a light jet, and the corresponding bj reconstruct a $W_{\rm had}$, while the second b is mistagged as a lepton [27]. Similarly for the 4ℓ signal there is a potential background from $t\bar{t} \to 2\ell 2\nu b\bar{b}$ production, where both b's are identified as leptons, although this background is suppressed by the square of the mistag rate.

The impact of the latter backgrounds critically depends on the actual detector performances. Although backgrounds of this type, originating from mistags, fakes, and detector effects, are likely to be relevant for the actual experimental analysis of the HWW production, their detailed analysis is beyond the scope of the present work.

G. Combination

We now combine the potential of the six channels previously discussed, reported in Table IX. Here we combine the final rates, after the optimization procedure, for the signal and total background for each final state, and the corresponding significances. Significances are for 3000 fb^{-1} of integrated luminosity. By summing in quadrature the significances of each individual channel, we get a total HWW signal significance of $3.6\sigma_S$ in the SM.

IV. ANOMALOUS HIGGS COUPLINGS

In this section we consider the possibility that the Higgs boson has non-SM couplings to W, Z bosons and fermions. In order to parametrize any deviation from the SM expectations, we introduce the set of scaling coefficients $C_{W,Z,f}$ defined as

$$C_W = \frac{g_{WWH}}{g^{\rm SM}_{WWH}}, \qquad C_Z = \frac{g_{ZZH}}{g^{\rm SM}_{ZZH}}, \qquad C_f = \frac{g_{ffH}}{g^{\rm SM}_{ffH}}, \quad (2)$$

where $g^{\rm SM}_{WWH}$, $g^{\rm SM}_{ZZH}$, and $g^{\rm SM}_{ffH}$ stand for the corresponding SM couplings. The C_Z and C_W parameters are constrained to be positive, while C_f can still assume negative values [13].

As discussed in Sec. I, anomalous Higgs couplings to SM weak gauge bosons and fermions can induce a violation of perturbative unitarity at some energy scale, which depends on the particular process considered. Perturbative unitarity can then be recovered by introducing new weakly coupled degrees of freedom with a mass spectrum at, or below, the unitarity breaking scale. In case no new elementary particle appears in the spectrum, the energy scale associated to the breaking of perturbative unitarity should be interpreted as the scale where interactions of the Higgs boson and longitudinal modes of vector gauge bosons become strong [28–30]. Unitarity is then expected to be recovered in a nonperturbative regime, by the exchange of strongly interacting composite resonances.

In case the Higgs couplings are modified without extending the SM content below the scale of the unitarity violation, total cross sections might increase with energy faster than the corresponding SM ones. A relevant example is provided by the single top production in association with a Higgs boson mediated by the subprocess $Wb \to Ht$ in pp collisions [17–19]. Its cross section is very sensitive not only to the magnitude of the ratio C_t/C_W but also to its sign, because of the strong destructive interference between the diagrams involving the Higgs coupling to the W and to the top-quark in the SM.

For the $pp \to HWW$ production, the cross section receives the largest contribution from the HWW coupling and has a milder dependence on the HZZ and Htt couplings.[3] In particular, the top-Yukawa coupling g_{ttH} enters through the subprocess $b\bar{b} \to HWW$ (see Fig. 1), which moderately contributes to the cross section with respect to the light-quark initiated subprocess $q\bar{q} \to HWW$. As for the HZZ coupling, it enters only through the s channel in all the subprocesses, and its impact is therefore subdominant with respect to the HWW-coupling one.

When assuming anomalous couplings, the energy scale of the partonic process must be held below the characteristic scale of unitarity violation in order to keep the cross section within the perturbative regime. In the $pp \to HWW$ case, this scale will mostly depend on the coefficients $C_{W,Z,t}$ and should tend to infinity for $C_{W,Z,t} \to 1$, which recovers the SM case. In order to determine the $pp \to HWW$ sensitivity to anomalous $C_{W,Z,t}$ coefficients in a perturbative regime, the effective partonic c.m. energy of the HWW system ($\lesssim$7 TeV at the LHC) must be kept below the energy scale of unitarity violations. To this purpose, we analyze below the relevant unitarity bounds

[3] We neglect any contribution from light-quark transitions to a top-quark (d, $s \to t$) via W exchange, the latter being strongly suppressed by off-diagonal terms of the Cabibbo-Kobayshi-Maskawa matrix.

associated to the partonic processes contributing to $pp \to HWW$ as a function of the anomalous Higgs couplings.

A. Analytical unitarity bounds

We now analyze the contribution to the $pp \to HWW$ cross section that comes from the b-quark initiated process

$$b(p_b)\bar{b}(p_{\bar{b}}) \to H(p_h)W^+(p_+)W^-(p_-), \tag{3}$$

where the quantities in parentheses label the corresponding particle momenta. A representative set of Feynman diagrams for the $b\bar{b} \to HWW$ is given in Fig. 1. This subprocess receives a large contribution from the top-quark Yukawa coupling [see Fig. 1(b)], and is also sensitive to anomalous Higgs couplings in both the W, Z and top-quark sectors. In the following, we will retain only the contribution from top-quark exchange diagrams, setting to zero the Yukawa couplings of lighter quarks since their effect does not significantly affect the present results.

The breaking of perturbative unitarity in the process in Eq. (3) is induced by the contributions of the vector-boson longitudinal polarizations. At high energy, the corresponding polarization vectors are approximated by

$$\epsilon_L^\mu(p_\pm) \approx \frac{p_\pm^\mu}{M_W}. \tag{4}$$

By retaining only the contribution of $W^\pm$ longitudinal polarizations in the relevant amplitude (labeled as $\mathcal{M}_{LL}$), one gets the asymptotic expression

$$\begin{aligned} i\mathcal{M}_{LL} = & \frac{2m_t^2}{v^3}(C_t - C_W) \\ & \times \bar{v}_{\bar{b}}\left(\frac{\not{p}_-}{(p_b - p_-)^2 - m_t^2} - \frac{\not{p}_+}{(p_{\bar{b}} - p_+)^2 - m_t^2}\right)P_L u_b \\ & + \frac{2M_Z^2}{v^3}(C_Z - C_W)\bar{v}_{\bar{b}}\left(\frac{\not{p}_+ - \not{p}_-}{s}\right)(2q_b s_w^2 + P_L)u_b, \end{aligned} \tag{5}$$

where u_b and $\bar{v}_{\bar{b}}$ are the spinors of the b and $\bar{b}$ quarks, respectively, v is the Higgs vacuum expectation value, $q_b = -1/3$ is the bottom-quark electromagnetic charge, and $P_L = (1-\gamma_5)/2$ is the left-handed chirality projector. M_Z and m_t are the Z and top-quark mass, respectively, while the b quark is assumed massless.

In the high-energy limit the kinematics is simplified by treating all the external particles as massless. Under this assumption, the phase space of the final state can be parametrized by the following dimensionless variables evaluated in the c.m. frame

$$\begin{aligned} (p_+ + p_-)^2 &\simeq s - 2\sqrt{s}E_H \equiv s y_H, \\ (p_H + p_+)^2 &\simeq s - 2\sqrt{s}E_- \equiv s y_-, \\ (p_H + p_-)^2 &\simeq s - 2\sqrt{s}E_+ \equiv s y_+, \end{aligned} \tag{6}$$

(with $y_+ + y_- + y_H = 1$) and three angular variables. E_i denotes the energy of the particle i. The rhs of Eq. (6) is explicitly evaluated by assuming the massless approximation.

The differential phase space, $d\Phi_3$, is then expressed as

$$d\Phi_3 = \frac{s}{32(2\pi)^3}\delta(1 - y_+ - y_- - y_H)dy_+ dy_- dy_H dz, \tag{7}$$

with $-1 \le z \le 1$, $0 \le y_i \le 1$, and z being the cosine of an angle between the initial (anti)particle and the final particle three-momenta. Two angular degrees of freedom have been integrated out. The asymptotic cross section is consequently

$$\sigma = \frac{(2\log(s/m_t^2) - 1)\delta_t^2 + 2\delta_t\delta_Z + \frac{1}{4}\delta_Z^2}{64(2\pi)^3 v^2}, \tag{8}$$

where, for left-handed fermions,

$$\begin{aligned} \delta_t &= \frac{2m_t^2}{v^2}(C_t - C_W) \approx 0.99(C_t - C_W), \\ \delta_Z &= \frac{2M_Z^2}{v^2}(2q_b s_w^2 + 1)(C_Z - C_W) \approx 0.23(C_Z - C_W), \end{aligned}$$

while for right-handed fermions $\delta_t = 0$, and in δ_Z the expression $2q_b s_w^2 + 1$ is replaced by $2q_b s_w^2$. The dominant contribution arises from the δ_t terms.

Given the above cross section, the unitarity bound can now be obtained by requiring [31]

$$\sigma \lesssim \frac{4\pi}{s}, \tag{9}$$

which holds under the assumption that the s-wave contribution dominates the elastic $b\bar{b} \to b\bar{b}$ scattering. The above inequality provides the tightest bound that perturbative unitarity can cast.

In order to simplify the analysis, we consider now two different scenarios for Higgs anomalous couplings. We first assume a universal rescaling of the Higgs couplings to weak gauge bosons by imposing $C_Z = C_W = C_V$. Secondly, we assume $C_f = C_W$ for the Higgs fermion couplings and vary the relative strength of C_Z and C_W, inducing in this way an explicit breaking of the custodial symmetry.

Then we obtain

(i) if $C_Z = C_W \equiv C_V$ [i.e., $\delta_Z = 0$ in Eq. (8)], the bound in Eq. (9) is given by

$$\frac{4\pi}{s} \ge \frac{m_t^4(C_t - C_W)^2}{16(2\pi)^3 v^6}\left(2\log\left(\frac{s}{m_t^2}\right) - 1\right); \tag{10}$$

(ii) if $C_t = C_W$ [which sets $\delta_t = 0$ in Eq. (8)], breaking the custodial symmetry by setting $C_Z \neq C_W$ yields

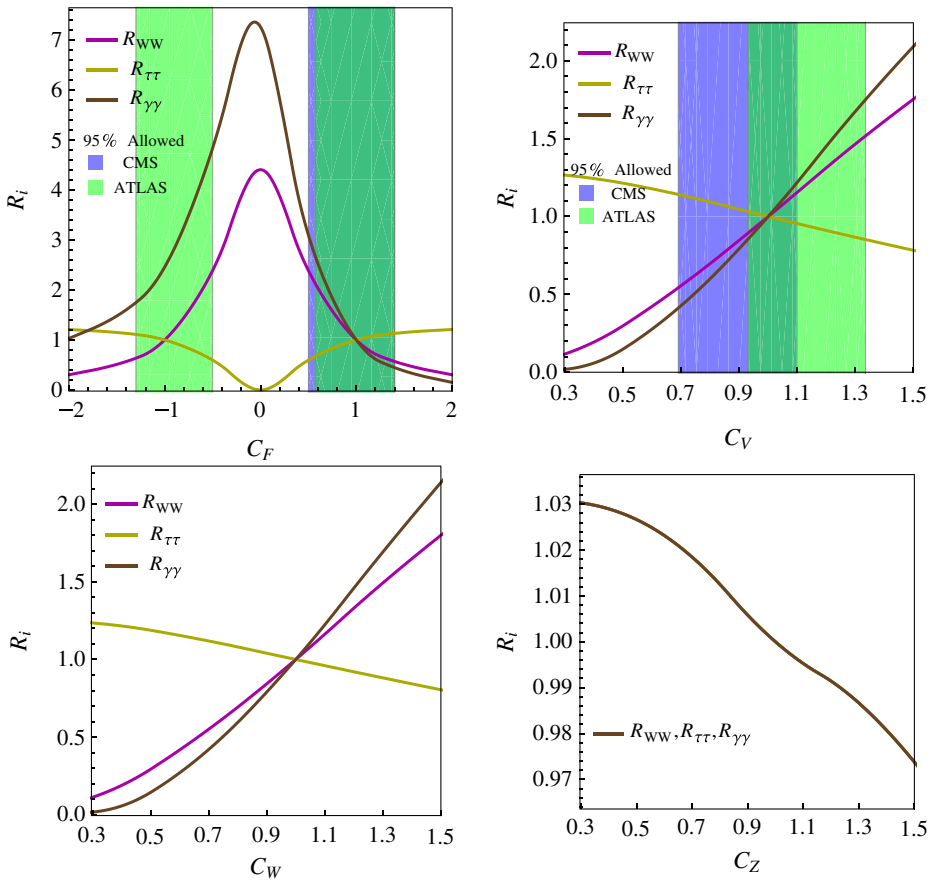

FIG. 2 (color online). Higgs boson BR's, normalized to their SM value, as a function of C_F, where $F = t, b, c, \tau\ldots$, for $C_V = 1$ (upper left panel), C_V, where $V = W, Z$, for $C_F = 1$ (upper right panel), C_W, for $C_{Z,F} = 1$ (lower left panel), and C_Z, for $C_{W,F} = 1$ (lower right panel). Here, $R_i = \mathrm{BR}_i/\mathrm{BR}_i^{\mathrm{SM}}$, where $\mathrm{BR}_i = \Gamma(H \to i)/\Gamma(H)_{\mathrm{tot}}$. The normalized BR's for $H \to W^+W^-$, $H \to \tau\tau$ and $H \to \gamma\gamma$ are shown by the magenta, yellow, and brown lines, respectively. In the upper plots, the blue and green areas show the regions allowed at 95% confidence level by the CMS and ATLAS experiments, respectively.

$$\frac{4\pi}{s} \geq \frac{m_Z^4 (C_Z - C_W)^2}{64(2\pi)^3 v^6} (2q_b s_w^2 + 1)^2. \quad (11)$$

By defining now the unitarity breaking (UB) energy scale, E_{UB}, as the specific value of $\sqrt{s}$ for which equalities hold in the above equations, we can see that in the first case E_{UB} is minimal when $C_t < 0$. In particular, setting $C_t = -C_V = -1$ we obtain

$$E_{\mathrm{UB}} \approx 14 \text{ TeV}. \quad (12)$$

For comparison, a similar value (namely $E_{\mathrm{UB}} \approx 9.3$ TeV) was found in [18] for the $Wb \to tH$ partonic process in single-top production in association with a Higgs boson, for $C_W = 1$ and $C_t = -1$. In the second case, given the actual bounds on the ratio C_Z/C_W [10], we can assume at most $|C_Z - C_W| \sim 0.2$. Correspondingly, the scale of unitarity violation brought by a maximal explicit custodial-symmetry breaking is

$$E_{\mathrm{UB}} \approx 4700 \text{ TeV}, \quad (13)$$

which is more than two orders of magnitude higher than the one induced by $C_t = -C_V = 1$.

In conclusion, we checked that all relevant unitarity bounds are well above the effective HWW partonic c.m. energies for $\mathcal{O}(1)$ (or less) variations of the $C_{W,Z,f}$ parameters. The partonic cross section for the HWW production at the LHC collision energies falls indeed in the perturbative regime (and therefore it is safely computable) for the $C_{W,Z,f}$ parameters within currently allowed experimental ranges [9–11].

B. Signal strengths and significances

We now discuss the sensitivity of the different $pp \to HWW$ channels analyzed in Sec. III to presently allowed variations of the $C_{W,Z,f}$ parameters. We first review the impact of such variations on the Higgs BR's. Then, we combine the latter information with the $pp \to HWW$ cross-section dependence on $C_{W,Z,f}$, obtaining in this way the sensitivity of production rates and significances to anomalous Higgs couplings for different HWW signatures.

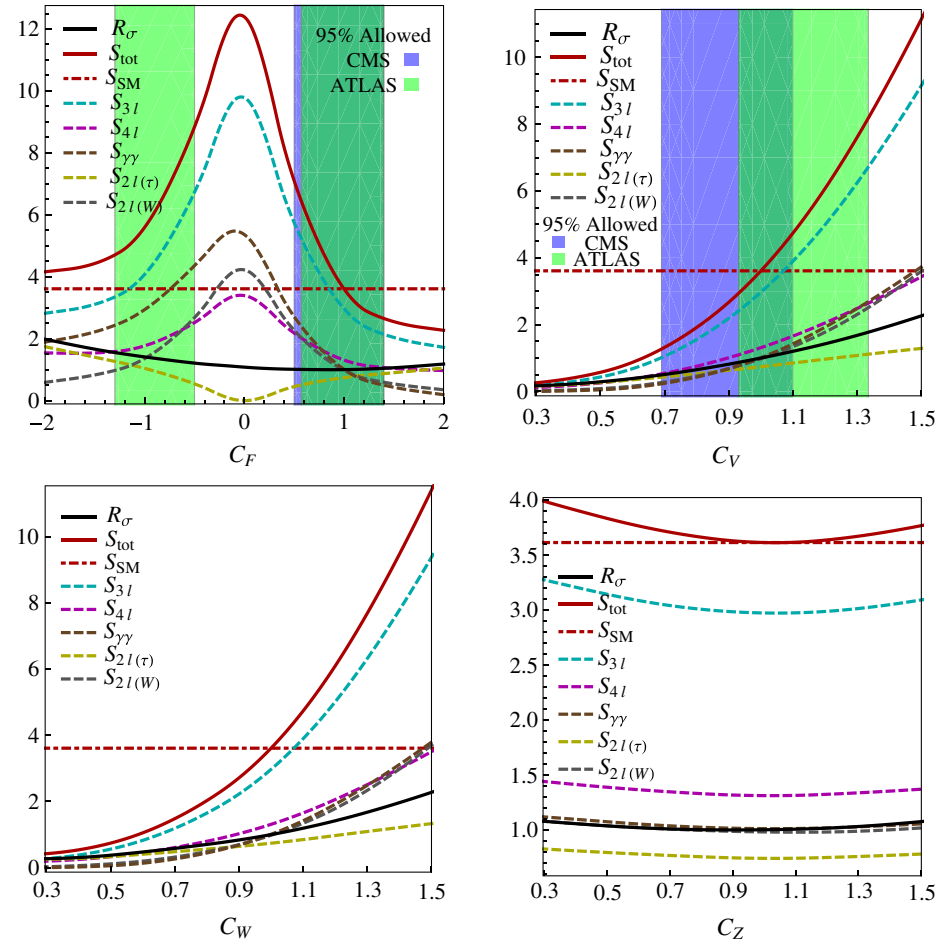

FIG. 3 (color online). The $pp \to WWH$ cross section, normalized to its SM value, $R_\sigma = \sigma/\sigma_{\rm SM}$ at 14 TeV (black solid line), and the combined signal significance (red solid line), corresponding to an integrated luminosity of 3000 fb^{-1}, as a function of C_F, for $C_V = 1$ (upper left panel), C_V, where $V = W, Z$, for $C_F = 1$ (upper right panel), C_W, for $C_{Z,F} = 1$ (lower left panel), and C_Z, for $C_{W,F} = 1$ (lower right panel). In the upper plots, the blue and green areas show the regions allowed at 95% confidence level by the CMS and ATLAS experiments, respectively. The individual significances of the five final states $[4\ell, 3\ell, \gamma\gamma, 2\ell(\tau\tau), 2\ell(WW^\star)]$, in units of standard deviations σ_S, are shown by the dashed magenta, cyan, brown, yellow, and gray lines, respectively. The horizontal red dot-dashed line shows for reference the combined signal significance in the SM.

In the following analysis, we assume that Higgs couplings to all fermions are modified by a universal rescaling coefficient C_F, defined as $C_F = C_f$ for all fermions f. As above, C_V is defined as a common rescaling factor for g_{WWH} and g_{ZZH}, namely $C_V = C_W = C_Z$.

In Fig. 2 we plot the Higgs BR's normalized to their SM values ($R_i = BR_i/BR_i^{\rm SM}$), for the decay channels relevant to our analysis, namely $H \to \gamma\gamma$, $H \to WW^*$, $H \to \tau\tau$, as a function of anomalous couplings in the range

$$-2 < C_F < 2, \qquad 0.3 < C_{W,Z,V} < 1.5. \tag{14}$$

In particular, in the top panels of Fig. 2, we plot the normalized BR's, R_i, versus C_F, for $C_V = 1$ (left), and C_V, for $C_F = 1$ (right), while in the bottom panels, the same quantities are plotted versus C_W, for $C_Z = C_F = 1$ (left), and C_Z, for $C_W = C_F = 1$ (right). The blue and light-green areas, in the top panel plots, label the regions allowed at 95% C.L. by the present CMS and ATLAS analysis, respectively, where the darker-green areas stand for their overlaps[4] [9–11].

One can see from the upper-left plot in Fig. 2 that the BR's for $H \to \gamma\gamma$ and WW^* ($H \to \tau\tau$) reach their maximum (minimum) at $C_F = 0$, which makes the Higgs total width minimal. Notice that the maximum of $R_{\gamma\gamma}$ is not set exactly at $C_F = 0$, since the corresponding decay width is not symmetric under a change in the C_t sign. This is due to the destructive (constructive) interference between the W- and top-quark contributions in the $H \to \gamma\gamma$ loop amplitude for

[4]In the bottom plots of Fig. 2, we do not report the experimental allowed regions, since these correspond to a different hypothesis with respect to the one used for the exclusion regions of couplings in the C_F/C_V plane adopted by CMS and ATLAS analysis.

positive (negative) values of C_F/C_W. On the other hand, the positive (negative) slope of R_i for $H \to WW^*, \gamma\gamma$ ($H \to \tau\tau$), versus C_V and C_W (in the upper-right and lower-left plots of Fig. 2, respectively), is just due to the rescaling property of the $H \to WW^*, \gamma\gamma$ decay widths versus the $C_{V/W}$ coupling. In the lower-left plot, we can see that all BR's plotted versus C_Z are degenerate, since the dependence on C_Z mainly affects the total Higgs width (i.e., a common normalization factor) in this case.

We now combine the latter results with the $pp \to HWW$ cross-section and signal-rate dependence on Higgs couplings, working out the potential of the individual five channels analyzed in Sec. III and their combination.

Figure 3 shows, as a function of anomalous $C_{f,V,W,Z}$, the $pp \to WWH$ total cross section R_σ normalized to its SM value (continuous black line), the corresponding significance S_i, expressed in standard deviations (σ_S), for the five signatures considered in Secs. III A, III B, III C, III D, III E (dashed colored lines), and their combined effect (continuous red line). The horizontal dashed-dot line corresponds to the SM combined significance for the five channels. All the significances reported in Fig. 3 are for a (14 TeV) LHC integrated luminosity of 3000 fb^{-1}.

We checked that in general the $pp \to HWW$ cross sections grow faster with energy when $C_{f,V}$ depart from the SM set-up, matching the expected unitarity-violation pattern. The most pronounced effect is obtained for negative top-Yukawa couplings, $C_t = C_F < 0$, that are more sensitive to the unitarity breaking regime than anomalous C_Z, as shown by Eqs. (10) and (11).

On the other hand, the cross section dependence on C_W (lower-left plot in Fig. 3) is mostly a consequence of the overall C_W^2 rescaling of the total cross sections, since Higgs radiation from a W boson gives the dominant contribution to the HWW production. Analogous conclusions hold (upper-right plot) for the cross section dependence on a common C_V rescaling factor. Quite large variations (up to 50%) of the total cross sections are expected for anomalous couplings in the 95% C.L. range allowed by present experiments.

We then combine in quadrature the expected HWW significances in different channels, versus $C_{V,F}$. Large enhancements can be obtained with respect to the SM signal sensitivity, for $C_{V,F}$ values presently allowed by LHC experiments (see Fig. 3), thanks to the combined effect of the cross section and BR's dependence on anomalous couplings. In particular, the significance versus C_F for the combined channels is maximal for $C_F \simeq 0$, reaching values up to $\sim 12\sigma_S$, as a consequence of the corresponding enhancements in the ratios $R_{\gamma\gamma,WW}$ (upper-left plot in Fig. 2). For $C_F \sim 0$, the most sensitive final states are three-leptons, and $\gamma\gamma$, followed by two-same-sign leptons. Within the allowed 95% C.L. regions, the highest combined significance, corresponding to $C_F \sim -0.5$, is about $\sim 9\sigma_S$.

For $C_F = 1$, upper-right and lower-left plots in Fig. 3 give different-channel significances versus C_V and C_W, respectively. The C_V and C_W dependence is mainly due to the naive rescaling property of the signal cross section and BR's with C_V and C_W. In particular, the maximum effect, corresponding to the largest allowed value $C_V \sim 1.3$, gives a $\sim 8\sigma_S$ significance for the combined channels. Analogous conclusions hold for the dependence on C_W (with $C_{Z,F} = 1$).

Finally, in Fig. 3, lower-right plot, we show the significance versus C_Z (with $C_{W,F} = 1$). The maximum enhancement in this case is obtained for the lower-edge $C_Z \sim 0.3$, with a significance $\sim 4\sigma_S$, and a modest 10% enhancement over the SM value, that falls down to a few percent for $0.8 \lesssim C_Z \lesssim 1.2$.

V. SUMMARY AND CONCLUSIONS

The discovery of the Higgs boson started a new phase in the experimental test of the electroweak symmetry breaking mechanism of the SM. Now it is indeed of utmost importance not only to study with high accuracy the Higgs production through the basic discovery channels, but also to explore lower-cross-section processes that can be sensitive to multiboson interactions. A typical example is given by the Higgs-boson pair production, which is the lowest-order process that probes at tree-level the trilinear term of the Higgs potential, and yet has a cross section of just 34 fb at the (14 TeV) LHC. Here we considered the largest-rate among the electroweak triboson production processes involving a Higgs boson in the final state, that is the associated production of a W pair and a Higgs boson. We analyzed (in a tree-level study) the cleanest experimental signatures corresponding to the HWW final state, that are either multilepton or diphoton resonances. The main backgrounds have been scrutinized. The most sensitive signature turns out to be a three lepton plus hadronic W final state that reaches a $3\sigma_S$ significance at the HL-LHC with 3000 fb^{-1}. Including other channels, we obtain a total $3.6\sigma_S$ significance in the SM.

We then carried out a first study of the $pp \to HWW$ sensitivity to possible Higgs anomalous couplings to vector bosons and fermions. We assumed a simple framework where a change in the fermion Higgs coupling sector is universal in fermion flavor. Regarding couplings to vector bosons, we assumed both a universal change in the W/Z coupling and the possibility of custodial symmetry breaking.

While the sensitivity to C_V in the cross section is driven by an approximate multiplicative factor C_V^2 in the total cross section, the dependence on C_F is mainly restricted to the $b\bar{b} \to HWW$ subprocess, whose amplitude presents, in the SM, non-trivial cancelation effects between the W and t quark radiation of a Higgs boson.

We also studied unitarity-breaking effects induced by anomalous Higgs couplings in the $q\bar{q} \to HWW$ amplitude behavior with c.m. scattering energy, and checked that the

corresponding cross section can be reliably computed at the LHC in the experimentally allowed range of Higgs anomalous couplings.

Note that, by the time the high-luminosity run of the LHC will start, our knowledge of Higgs boson couplings will have widely been enlarged with respect to the present one [20,21]. In case some deviation from the SM expectations in the Yukawa and/or vector boson sectors will have been observed by then, our preliminary study shows that the HWW production mode could be an extra valuable channel to clarify the emerging picture. Furthermore, even in a scenario where the SM picture is apparently confirmed, the HWW production could probe higher-dimensional operators by which higher-cross-section processes are moderately affected. We leave to further work the assessment of the HWW potential in this case. We finally stress that a more reliable evaluation of the $pp \to HWW$ potential for testing the Higgs-boson properties at the LHC will require a more realistic simulation of both theoretical higher-order effects and the experimental apparatus impact.

ACKNOWLEDGMENTS

We thank M. Raidal for useful discussions. E. G. would like to thank the PH-TH division of CERN for its kind hospitality during the preparation of this work. This work was supported by the ESF Grants No. 8499, No. 8943, No. MTT8, No. MTT59, No. MTT60, No. MJD140, No. MJD435, No. MJD298, No. MJD387, by the recurrent financing SF0690030s09 project and by the European Union through the European Regional Development Fund.

[1] G. Aad *et al.* (ATLAS Collaboration), Phys. Lett. B **716**, 1 (2012).
[2] S. Chatrchyan *et al.* (CMS Collaboration), Phys. Lett. B **716**, 30 (2012).
[3] M. Baillargeon, F. Boudjema, F. Cuypers, E. Gabrielli, and B. Mele, Nucl. Phys. **B424**, 343 (1994).
[4] K. Cheung, Phys. Rev. D **49**, 6224 (1994).
[5] A. Djouadi, Phys. Rep. **457**, 1 (2008).
[6] S. Mao, M. Wen-Gan, Z. Ren-You, G. Lei, W. Shao-Ming, and H. Liang, Phys. Rev. D **79**, 054016 (2009).
[7] B. W. Lee, C. Quigg, and H. B. Thacker, Phys. Rev. D **16**, 1519 (1977).
[8] T. Appelquist and M. S. Chanowitz, Phys. Rev. Lett. **59**, 2405 (1987); **60**1589(E) (1988).
[9] ATLAS Collaboration, Report No. ATLAS-CONF-2012-127.
[10] ATLAS Collaboration, Report No. ATLAS-CONF-2013-034.
[11] CMS Collaboration, Report No. CMS-PAS-HIG-12-045; CMS Collaboration, Report No. CMS-PAS-HIG-13-005.
[12] E. Gabrielli and B. Mele, Phys. Rev. D **82**, 113014 (2010); **83**079901(E) (2011).
[13] S. E. Hedri, P. J. Fox, and J. G. Wacker, arXiv:1311.6488.
[14] T. M. P. Tait and C.-P. Yuan, Phys. Rev. D **63**, 014018 (2000).
[15] F. Maltoni, K. Paul, T. Stelzer, and S. Willenbrock, Phys. Rev. D **64**, 094023 (2001).
[16] V. Barger, M. McCaskey, and G. Shaughnessy, Phys. Rev. D **81**, 034020 (2010).
[17] S. Biswas, E. Gabrielli, and B. Mele, J. High Energy Phys. 01 (2013) 088.
[18] M. Farina, C. Grojean, F. Maltoni, E. Salvioni, and A. Thamm, J. High Energy Phys. 05 (2013) 022.
[19] S. Biswas, E. Gabrielli, F. Margaroli, and B. Mele, J. High Energy Phys. 07 (2013) 073.
[20] CMS Collaboration, arXiv:1307.7135.
[21] ATLAS Collaboration, arXiv:1307.7292.
[22] https://twiki.cern.ch/twiki/bin/view/LHCPhysics/HiggsEuropeanStrategy2012.
[23] J. Alwall, M. Herquet, F. Maltoni, O. Mattelaer, and T. Stelzer, J. High Energy Phys. 06 (2011) 128.
[24] J. Pumplin, D. R. Stump, J. Huston, H. L. Lai, P. M. Nadolsky, and W. K. Tung, J. High Energy Phys. 07 (2002) 012.
[25] A. Papaefstathiou, L. L. Yang, and J. Zurita, Phys. Rev. D **87**, 011301 (2013).
[26] T. Sjostrand, S. Mrenna, and P. Z. Skands, J. High Energy Phys. 05 (2006) 026.
[27] Z. Sullivan and E. L. Berger, Phys. Rev. D **82**, 014001 (2010).
[28] M. S. Chanowitz, M. Golden, and H. Georgi, Phys. Rev. Lett. **57**, 2344 (1986).
[29] M. S. Chanowitz, M. Golden, and H. Georgi, Phys. Rev. D **36**, 1490 (1987).
[30] A. Dobado, M. J. Herrero, J. R. Pelaez, E. Ruiz Morales, and M. T. Urdiales, Phys. Lett. B **352**, 400 (1995).
[31] D. A. Dicus and H.-J. He, Phys. Rev. D **71**, 093009 (2005).